Nitrogen Recycling and Remobilization Are Differentially Controlled by Leaf Senescence and Development Stage in Arabidopsis under Low Nitrogen Nutrition[1]

Céline Diaz, Thomas Lemaître, Aurélie Christ, Marianne Azzopardi, Yusuke Kato, Fumihiko Sato, Jean-François Morot-Gaudry, Frédérik Le Dily, and Céline Masclaux-Daubresse*

Unité de Nutrition Azotée des Plantes, UR511, INRA, F–78000 Versailles, France (C.D., T.L., A.C., M.A., J.-F.M.-G., C.M.-D.); Division of Integrated Life Science, Graduate School of Biostudies, Kyoto 606–8502, Japan (F.S.); and UMR INRA-UCBN, Ecophysiologie Végétale, Agronomie et Nutritions, Université de Caen, F–14000 Caen, France (F.L.D.)

Five recombinant inbred lines (RILs) of Arabidopsis (*Arabidopsis thaliana*), previously selected from the Bay-0 × Shahdara RIL population on the basis of differential leaf senescence phenotypes (from early senescing to late senescing) when cultivated under nitrogen (N)-limiting conditions, were analyzed to monitor metabolic markers related to N assimilation and N remobilization pathways. In each RIL, a decrease of total N, free amino acid, and soluble protein contents with leaf aging was observed. In parallel, the expression of markers for N remobilization such as cytosolic glutamine synthetase, glutamate dehydrogenase, and CND41-like protease was increased. This increase occurred earlier and more rapidly in early-senescing lines than in late-senescing lines. We measured the partitioning of ^{15}N between sink and source leaves during the vegetative stage of development using ^{15}N tracing and showed that N remobilization from the source leaves to the sink leaves was more efficient in the early-senescing lines. The N remobilization rate was correlated with leaf senescence severity at the vegetative stage. Experiments of ^{15}N tracing at the reproductive stage showed, however, that the rate of N remobilization from the rosettes to the flowering organs and to the seeds was similar in early- and late-senescing lines. At the reproductive stage, N remobilization efficiency did not depend on senescence phenotypes but was related to the ratio between the biomasses of the sink and the source organs.

Leaf senescence is a long developmental process leading to death. In Arabidopsis (*Arabidopsis thaliana*), leaf senescence onset starts as leaf expansion stops (Buchanan-Wollaston et al., 2003; Diaz et al., 2005) through the induction of a series of metabolic changes allowing nutrient recycling and remobilization. Because plants are static and most of the time nutrients are limited, Leopold (1961) proposed that leaf senescence was selected through evolution to allow plants to improve nutrient economy and to survive upon starvation. Indeed, nitrogen (N) depletion is known to accelerate leaf senescence and to increase N recycling and mobilization (Schulze et al., 1994). Through recycling the endogenous nutrients from the senescing leaves, plants can better support the growth of younger leaves and reproductive organs under nutrient-limiting nutrition (for review, see Masclaux-Daubresse et al., 2008).

Mechanisms and enzymatic processes for N mobilization during leaf senescence have been investigated in numerous plant models (Bernhard and Matile, 1994; Masclaux et al., 2000; Martin et al., 2005; Cabello et al., 2006). Rubisco is the main leaf N storage protein, and the degradation of this enzyme during senescence has been widely studied even though Rubisco degradation is still poorly understood. Rubisco proteolysis could be initiated by the deleterious effects of reactive oxygen species (Ishida et al., 1998). Afterward, the senescence-induced aspartic protease CND41, encoded by the nuclear genome and localized specifically to the chloroplast, could degrade Rubisco. In vitro analysis confirmed that CND41 showed a Rubisco proteolytic activity at physiological pH values (Nakano et al., 1997; Kato et al., 2004; Fig. 1). However, CND41 could not act on Rubisco unless its structure was denatured. Therefore, active Rubisco in the chloroplast would be resistant to CND41-catalyzed degradation until leaf senescence is under way. CND41 homologs have been identified in Arabidopsis that might also be responsible for the regulation of Rubisco turnover and senescence. Rubisco degradation certainly releases numerous free

[1] This work was supported by the Centre Technique Interprofessionnel des Oléagineux Metropolitains (http://www.cetiom.fr) and INRA Department of Biology (to C.D.), and by the University of Versailles Saint Quentin en Yvelines (France; T.L. was ATER).

* Corresponding author; e-mail masclaux@versailles.inra.fr.

The author responsible for distribution of materials integral to the findings presented in this article in accordance with the policy described in the Instructions for Authors (www.plantphysiol.org) is: Céline Masclaux-Daubresse (masclaux@versailles.inra.fr).

www.plantphysiol.org/cgi/doi/10.1104/pp.108.119040

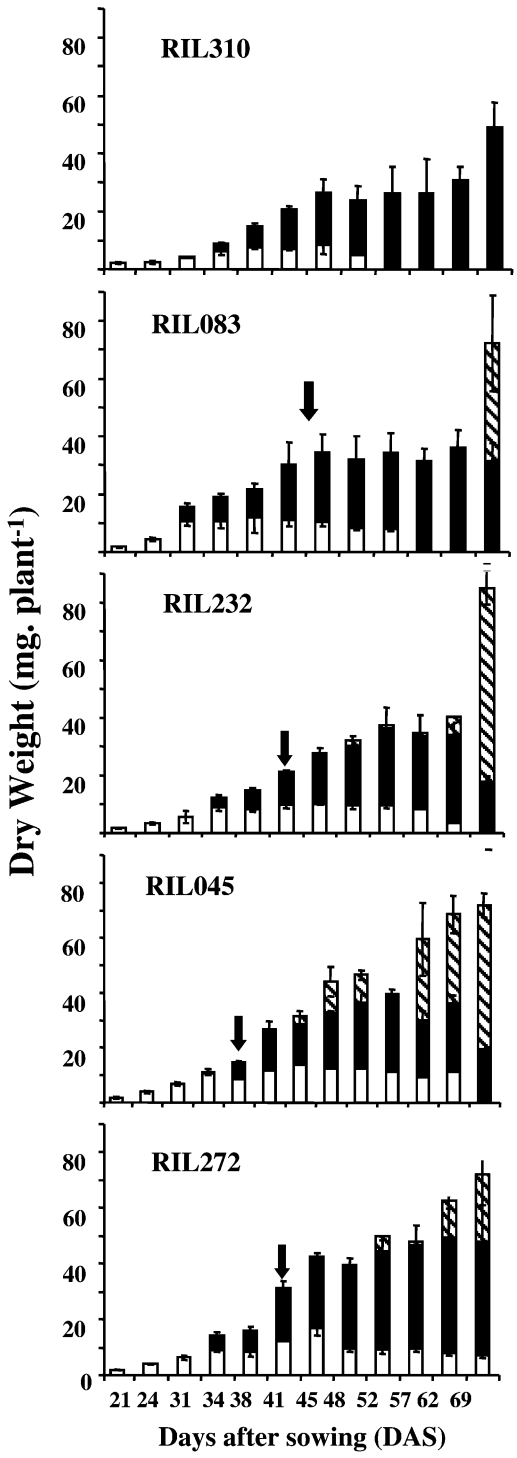

Figure 1. Comparison of DW (milligrams per plant) of the 6FL (white bars), NL (black bars), and flowering stems (hashed bars) of RIL310, RIL083, RIL232, RIL045, and RIL272. Means and SES are presented, $n = 4$ to 6. The arrows indicate the flowering time.

amino acids available for phloem loading and other interconversions. The way by which amino acids are loaded to the phloem of senescing leaves for translocation is poorly documented (van der Graaff et al., 2006). One possibility is that amino acids would be interconverted to increase the synthesis of amino acids dedicated to transport, like Gln and Asn. Indeed, in tobacco (*Nicotiana tabacum*), it has been shown that the cytosolic Gln synthetase (GS1) and the mitochondrial Glu dehydrogenase (GDH) are induced as the primary N-assimilating enzymes decrease with aging (Masclaux et al., 2000). Through the catabolism of Glu, GDH provides ammonium as a substrate for neosynthesis of Gln by cytosolic GS1 (Masclaux-Daubresse et al., 2006). Both GS1 and GDH enzymes are mainly located in the roots. However, during senescence, GS1 protein is detected in both leaf mesophyll and companion cells (Brugière et al., 2000). The GS1 and GDH enzymes are octameric and hexameric proteins, respectively. Genes encoding their different subunits belong to multigenic families, and in Arabidopsis, five genes have been isolated for GS1 (*gln1.1–gln1.5*) and three genes (*gdh1–gdh3*) for the NADH-dependant GDH. From molecular physiology and gene-expression profiling, it appears that *gln1.1*, *gln1.2*, *gln1.4*, and *gdh2* belong to the Senescence Associated Genes family (Bernhard and Matile, 1994; Guo et al., 2004). However, the precise role of these genes in the N remobilization process still remains to be investigated in Arabidopsis.

In a previous report, the extent and the variability of leaf senescence in Arabidopsis were characterized using five genotypes from the Bay-0 × Shahdara recombinant inbred line (RIL) population that have been selected for their differential leaf lifespan, yellowing-symptom earliness, and intensity (Diaz et al., 2005). A metabolic profiling of aging leaves from the five RILs showed that metabolite contents were similarly modified throughout aging regardless of the genetic background of the RILs (Diaz et al., 2005). Age-related modifications, however, occurred earlier and were more pronounced in the early-senescing lines than in the late-senescing lines. From this study, it was shown that the quantities of hexoses, Suc, starch, and individual amino acids in leaves change with aging and depend on the senescence severity. In particular, γ-aminobutyrate, Leu, Ile, Tyr, and Arg accumulate to a greater extent during leaf aging and in the leaves of early-senescing lines compared to those of late-senescing lines. At the same time, Glu and Asp decrease more rapidly in early-senescing lines with aging. This study then showed that transaminating activities are certainly differentially expressed during leaf aging and senescence. The amino acids do not all play the same role in plant metabolism and are not mobilized with the same efficiency. All these results lead us to address the question of the leaf N remobilization efficiency (NRE) in the five RILs.

In this report, the expression of the N remobilization enzymatic and molecular markers have been monitored during leaf aging in the five genetic backgrounds chosen previously by Diaz et al. (2005). The aim was to determine if the mechanisms for N remobilization and their regulation are similar in Arabidopsis and in other plant species and if N remobilization depends on leaf

aging and leaf-yellowing severity. To determine if total N export is correlated with leaf senescence and/or N remobilization markers, we determined different carbon and N pools and measured N fluxes using ^{15}N tracing.

RESULTS

Comparison of the Biomass of Five RILs Showing Differential Senescence Patterns

Diaz et al. (2005) characterized the Arabidopsis RILs on the basis of leaf senescence phenotypes. RIL310 is the earliest senescing line, RIL083 and RIL232 are early senescing, while RIL045 and RIL272 are late-senescing lines. The six first leaves (6FL) of the rosettes that have emerged concomitantly for all the RILs were used to compare the effect of aging on N metabolism between genotypes. Rosettes were dissected to isolate and collect the 6FL and the new leaves (NL), which are the pool of leaves that have emerged after the 6FL. While the biomass of the 6FL depends only on the biomass of each leaf, the biomass of the NL depends on both the number of leaves that have emerged with time and their growth rate. The 6FL can be considered as a source of N mobilization for the NL that will in turn be a further source for the flowering stems.

The dry weight (DW) of the 6FL changed according to a bell-shaped curve (Fig. 1) for all the RILs. The 6FL DW stabilized when leaves attained maturity, then the 6FL DW decreased. This decrease was observed earlier and was more rapid for the early-senescing lines than for the late-senescing lines. The DW of the NL also changed according to a bell-shaped curve, but the decreasing phase of this curve was not related to the senescence phenotype of the line but to the emergence of the flowering bud. Interestingly, the total rosette DW (6FL-DW + NL-DW) was higher in the late-senescing lines (RIL272, 45 mg, and RIL045, 40 mg) than in the early-senescing lines (RIL310, 30 mg, and RIL083, 30 mg), thus illustrating the negative correlation between rosette dry matter and leaf yellowing that was found previously by Diaz et al. (2006) when studying the variation of N use efficiency and senescence traits on the whole RIL population.

Comparison of the Chlorophyll and Starch Contents in the 6FL and the NL of the Five RILs

As previously described by Diaz et al. (2005), the total chlorophyll decreased with leaf aging earlier and more rapidly in the 6FL of early-senescing lines than in the 6FL of late-senescing lines (Fig. 2A). In the 6FL, the extent of chlorophyll decrease paralleled the decrease of starch concentration for all of the lines, except RIL045 (Fig. 2B). In the NL, the concentration of chlorophyll was surprisingly higher in the early-senescing lines than in the late-senescing lines (Fig. 2C), suggesting that the NL chlorophyll concentration could compensate the higher loss in the 6FL of the same plant. By contrast, the starch concentration in the NL was higher in the late-senescing lines (Fig. 2D), suggesting that the

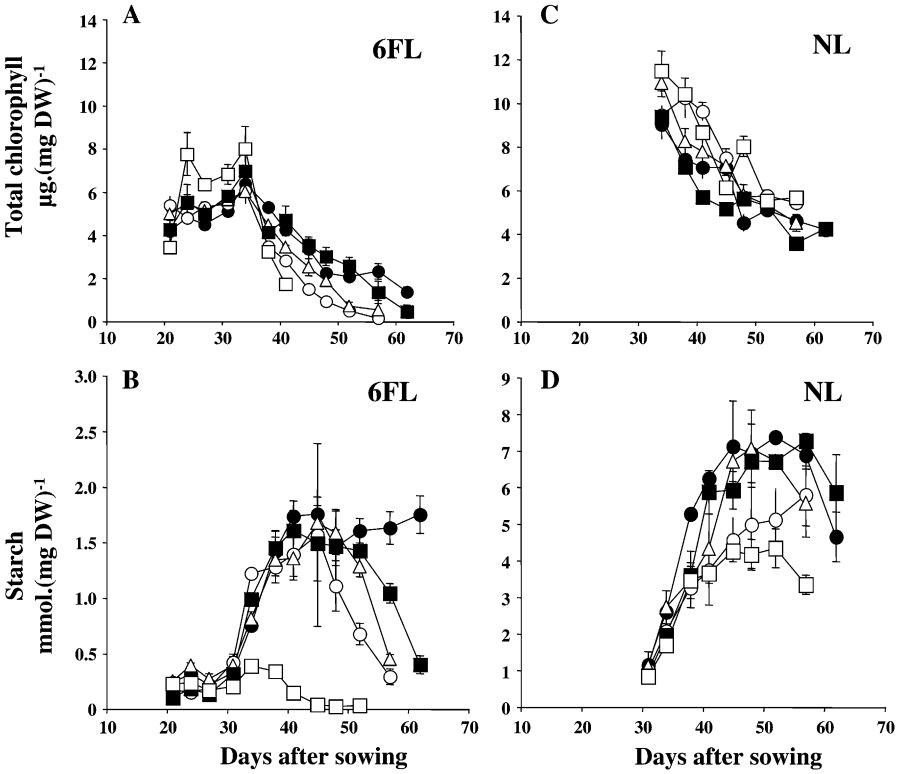

Figure 2. Total chlorophyll (A and C) and starch (B and D) concentrations in the 6FL (A and B) and the NL (C and D) of RIL310 (white squares), RIL083 (white circles), RIL232 (white triangles), RIL045 (black circles), and RIL272 (black squares). Means and SES are presented, $n = 3$.

photosynthetic carbon assimilation was better in the late-senescing lines.

Total Protein Content, Total Amino Acid Content, and Total N Amount Decreased in the 6FL and the NL of the Five RILs

The concentration of total N decreased with rosette aging in a similar way for all the RILs (Fig. 3, A and B). This decrease occurred at 24 d after sowing (DAS) in the 6FL and 35 DAS in the NL. Surprisingly, the decrease of N in the 6FL was not delayed in the late-senescing lines compared to early-senescing lines. In the NL, the N decrease was less pronounced in RIL310 than in other lines.

Total N can be distinguished in structural N and remobilizable N. Amino acids and soluble proteins are N-remobilizable pools. With aging, both free amino acids and soluble protein concentrations decreased in NL and 6FL (Fig. 3, C–F). In the 6FL, the decrease in total protein appeared earlier for the hyper-senescing RIL310 line and was slightly higher for all the early-senescing lines compared to the late-senescing lines after 50 DAS (Fig. 3C). The decrease of amino acid concentration in the 6FL was also similar in the early- and late-senescing lines, except in RIL310 that remained with higher amino acid concentration (Fig. 3E).

In the NL, the soluble protein (Fig. 3D) and the free amino acid concentrations (Fig. 3F) were higher in the early-senescing lines than in the late-senescing lines, showing an opposite trend as that observed for sugars (Diaz et al., 2005; Fig. 2D).

Changes in N Enzyme Activities in the 6FL of the Five RILs during Aging

It has been widely reported that primary N assimilation enzymes are down-regulated with leaf aging, while N remobilization enzymes are induced (Masclaux et al., 2000). Therefore, we measured GS, GDH, and nitrate reductase (NR) activities on the 6FL of the five RILs. As expected, the NR and GS activities decreased with aging (Fig. 4, A and B), whereas GDH activity increased (Fig. 4, C and D). However, time courses of NR activity decrease and GDH activity increase were not different between the early- and late-senescing RILs. By contrast, the total GS activity decreased earlier and more rapidly in the 6FL of early-senescing lines than in those of late-senescing lines.

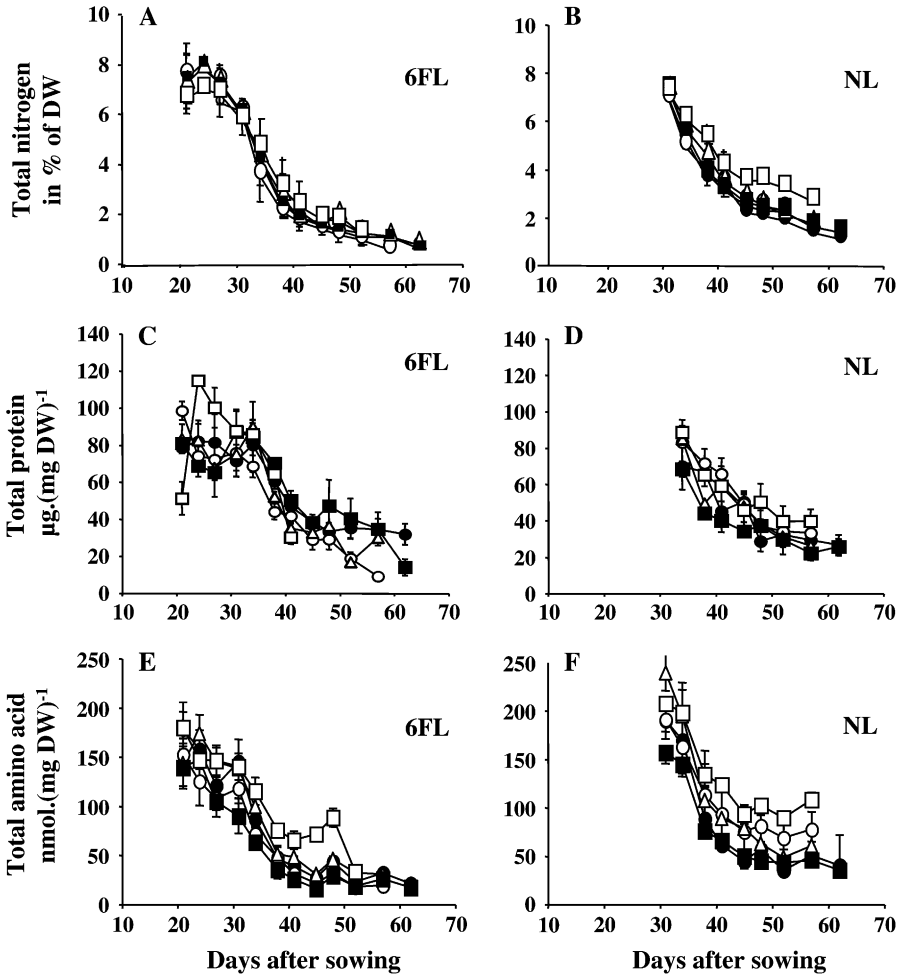

Figure 3. Total N concentration (A and B), soluble protein concentration (C and D), and free amino acid concentration (E and F) in the 6FL (A, C, and E) and the NL (B, D, and F) of RIL310 (white squares), RIL083 (white circles), RIL232 (white triangles), RIL045 (black circles), and RIL272 (black squares). Means and SES are presented, $n = 3$.

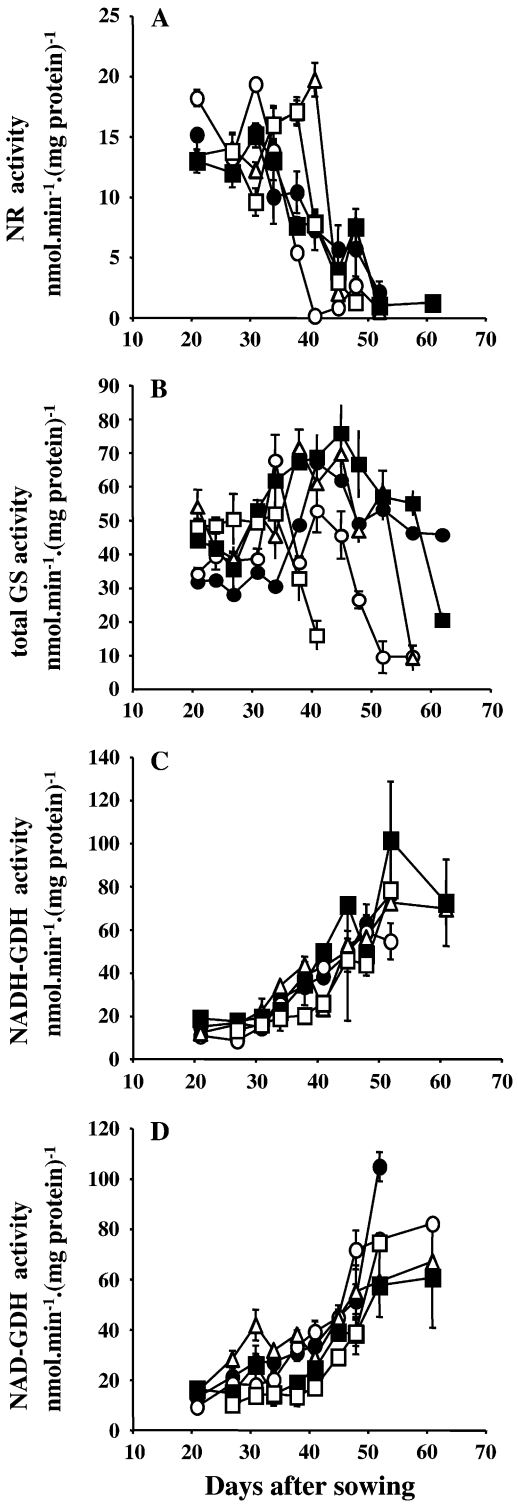

Figure 4. Determination of NR (A), GS (B), and NADH-dependent (C) and NAD-dependent (D) Glu dehydrogenase in extracts of the 6FL of RIL310 (white squares), RIL083 (white circles), RIL232 (white triangles), RIL045 (black circles), and RIL272 (black squares). Means and SES are presented, $n = 3$.

Changes in GS, Rubisco, and CND41-Like Protein Contents in the 6FL of the Five RILs

We measured the abundance of GS1, GS2, Rubisco, and CND41 proteins by gel staining and antibodies. The amount of GS1 protein increased with aging for all the RILs, whereas the amount of GS2 protein decreased (Fig. 5A). The increase in GS1 protein was sharper in the 6FL of RIL310 at 41 and 45 DAS. Rubisco content decreased with leaf aging for all the lines, but earlier and more rapidly in the 6FL of RIL310 and RIL083 (Fig. 5B). Antibodies raised against the tobacco CND41 chloroplastic aspartic protease (Kato et al., 2004) were used to detect a potential CND41-like protein in Arabidopsis. Very interestingly, the signal detected with the CND41 antibodies was higher in the early-senescing lines (Fig. 5C). The CND41 signal remained very low in RIL045 and was almost undetectable in the 6FL of RIL272.

Change in the N Enzyme mRNA Contents in the 6FL of the Five RILs

Total RNA was extracted from the 6FL of the RILs. These leaves were senescing earlier in RIL310, RIL232, and RIL083 than in RIL045 and RIL272. Because RNA degraded during senescence, the content and quality of the RNA extracted from the first leaves of these lines did not allow us to properly detect transcripts after 41, 48, and 52 DAS for RIL310, RIL083, and RIL232, respectively. This explains why results are likely to be incomplete for these lines.

The expression of the chlorophyll *a/b*-binding protein gene (*cab*) was used as a marker for senescence gene down-regulation. The decrease in *cab* mRNA expression occurred earlier in the 6FL of RIL310 (27 DAS) and RIL083 (31 DAS) than in the 6FL of RIL232, RIL045, and RIL272 (34 DAS). The *cab* mRNA remained detectable in RIL272 and RIL045 late, until 52 and 57 DAS, respectively (Fig. 6).

By comparison with *cab*, both *nia* and *gln2* mRNA, encoding NR and GS2 proteins, respectively, decreased with aging. The amount of *nia* and *gln2* mRNA decreased earlier and to a greater extent in early-senescing lines than in late-senescing lines. By contrast, *gln1.1* and *gln1.2* (both encoding GS1 proteins), *gad2* (encoding a Glu decarboxylase isoform), and *gdh2* (encoding GDH) mRNA levels increased with leaf aging earlier and to a greater extent in the early-senescing lines than in the late-senescing lines (Fig. 6).

Comparison of the N Fluxes and N Remobilization during the RIL Development Using ^{15}N Tracing

To determine to what extent N is mobilized during plant development and to compare this trait between the five RILs, labeling experiments were carried out as described in ''Materials and Methods.'' Three different labeling protocols were designed to determine: (1) the

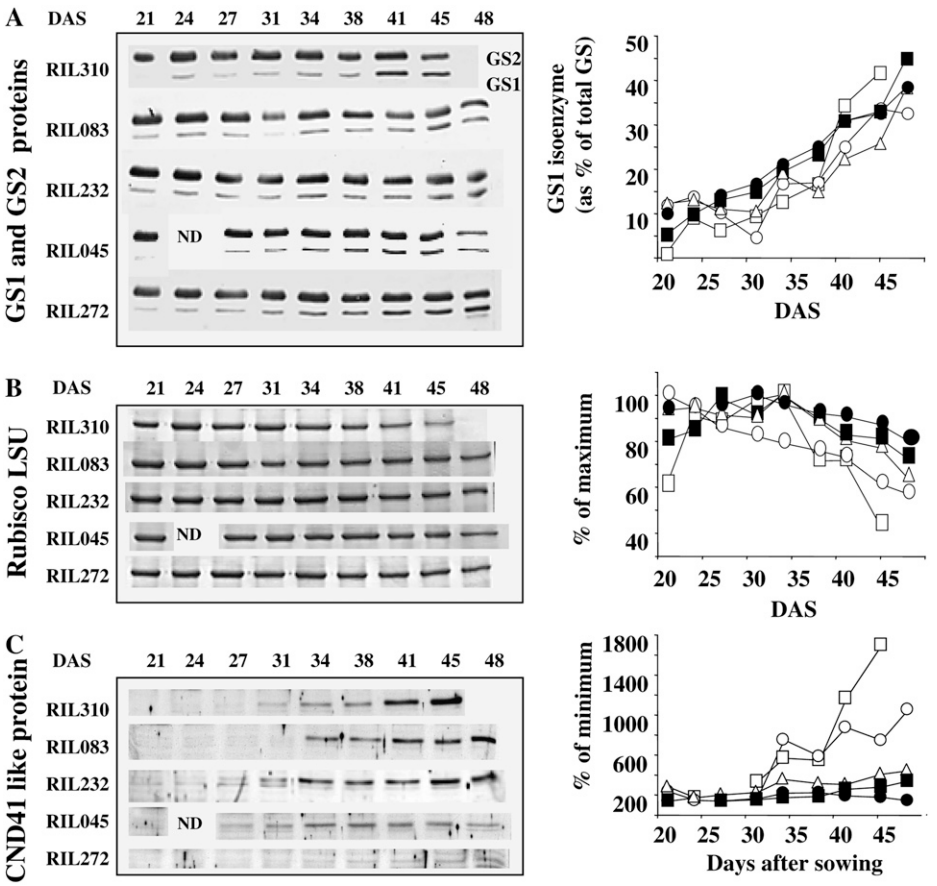

Figure 5. Analysis of the GS2 and GS1 protein content (A), Rubisco protein content (B), and CND41-like protein content (C) in extracts of the 6FL of the five RILs. Western blots and gel staining are presented. Quantifications of the signals and relative values are shown for RIL310 (white squares), RIL083 (white circles), RIL232 (white triangles), RIL045 (black circles), and RIL272 (black squares). Equal amounts of proteins have been loaded in each lane (see "Materials and Methods").

level of ^{15}N remobilization from leaf to leaf during the vegetative phase of the rosette growth (experiment [Exp.] 1); (2) the level of ^{15}N remobilization from rosette to flowering organs during the reproductive phase (Exp. 2); and (3) the level of ^{15}N remobilized for seed filling (Exp. 3).

In Exp. 1, we used the 11 first leaves (11FL) of the rosettes as source leaves rather than the 6FL as it was done with the compost-grown plants, because rosettes grown upon hydropony developed more slowly and were smaller. For that reason, the 2 to 3 mg DW needed to perform N measurements cannot be obtained from the 6FL at time 0 (T0). Because the five RILs developed the 11FL quite simultaneously in hydropony, this batch of leaves was chosen as source leaves labeled until T0. The ^{15}N fluxes from the 11FL, labeled during the pulse period, to the NL emerged during the chase period, were illustrated by the partition of ^{15}N at the end of the pulse period (T0) and at T1, 10 d later. Between T0 and T1, six to seven NL emerged. Because these NL appeared and developed during the chase period, the ^{15}N they contain can only come from the remobilization of the ^{15}N absorbed during the pulse period and assimilated in the roots and in the 11FL before the end of the pulse period. The measurement of the total ^{15}N quantity (Q) in each organ at T0 and T1 allowed us to calculate for the whole plant (wp) the quantities of ^{15}N at T0 (Qwp_{T0}) and at T1 (Qwp_{T1}). For all the RILs, Qwp_{T0} is equal to Qwp_{T1} (data not shown), showing that there was no loss of ^{15}N during the chase period.

At T0, the partitioning [P%(^{15}N) = Qi/Qwp] of ^{15}N in roots and shoots (i.e. 11FL) was quite similar between the five RILs (Fig. 7, A and B). Approximately 15% of the ^{15}N has been assimilated in the roots during the pulse period, while the major part (85%) was incorporated in the 11FL. The determination of P% in the roots, the 11FL, and the NL at T1 showed that ^{15}N has been mobilized from the roots and from the 11FL to the NL. Remobilization from the 11FL was higher than from the roots for all the RILs (Fig. 7, A and B). Moreover, the percentage of ^{15}N exported from the 11FL to the NL during the chase period was significantly higher for the early-senescing lines than for the late-senescing lines, thus showing that the extent of ^{15}N remobilization is linked to leaf senescence intensity (Fig. 7, B and C). The early-senescing RIL310, RIL083, and RIL232 have remobilized 16%, 10%, and 12% of N, respectively, from 11FL to NL between T0 and T1, while the late-senescing RIL045 and RIL272 mobilized 5% and 7% of N, respectively, during the same period of time.

In Exp. 2, the flux of ^{15}N from the whole rosette and the roots to the flowering stem and reproductive organs was investigated. Because only RIL083 and

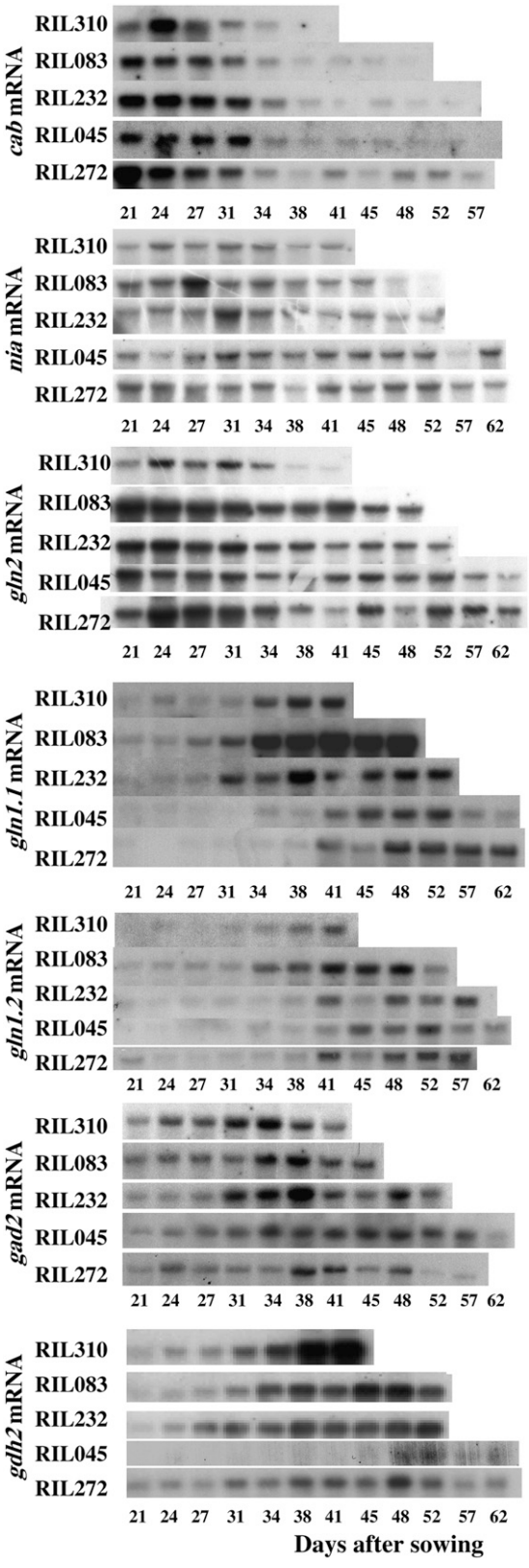

Figure 6. Changes in the steady-state levels of transcripts for the *cab* senescence marker, *nia*, *gln2*, *gln1.1* and *gln1.2*, *gad2*, and *gdh2* in the 6FL with an 18S rRNA probe used as a control for loading standardization (not shown).

RIL272 (Diaz et al., 2005) flowered in the same time, these lines were chosen for this experiment. Roots and rosettes were labeled with $^{15}NO_3^-$ until the emergence of the flowering bud (T0), which occurred at 59 DAS. At T0, for each line, three labeled plants were separated as root and rosette. During the chase period, plants were collected at 66 DAS (T1) and 88 DAS (T2). The newly appeared organs between T0, T1, and T2 were then separated as cauline leaves, primary (I) and secondary (II) stems, siliques, and flowers. For all the lines, it was verified that $Qwp_{T0} = Qwp_{T1} = Qwp_{T2}$ (data not shown). The partitioning of ^{15}N and the level of ^{15}N mobilized is presented in Table I. At T0, the partitioning of ^{15}N in the roots was higher for RIL272 than for RIL083 (25% versus 20%). This difference was

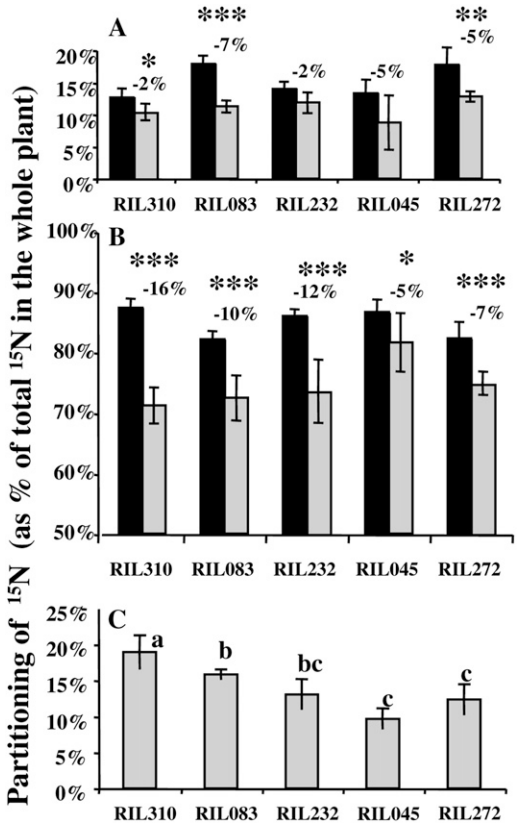

Figure 7. Change of the partitioning of ^{15}N in the roots (A), first leaves (B), and NL that appeared during the chase period (C). At T0 (dark bars, end of the labeling period), only roots and 11FL have developed. At T1 (gray bars, T0 + 10 d), which is the end of the chase period, six to seven NL have emerged. Calculation of partitioning of ^{15}N in roots and 11FL at T1, and in roots, 11FL, and NL at T2 is described in ''Materials and Methods.'' Values are the means of six individual plants, SES are presented. The percentage of N mobilized from roots and 11FL to the NL between T0 and T1 is mentioned on the graph, on the top of the bars. The probability that the differences between T0 and T1 (between dark and gray bars) was not significant was estimated using ANOVA and is indicated as such: *, $P < 0.05$; **, $P < 0.01$; ***, $P < 0.001$. From the data of partitioning of ^{15}N in the NL (C), three groups, a, b, and c, have been identified to be significantly different (Fischer test [LSD] P value >0.05).

Table I. *Evolution of the partitioning of ^{15}N, P%(^{15}N), in the different organs of early-senescing line RIL083 and the late-senescing line RIL272 between the end of the labeling period (T0, 59 DAS) and two time intervals of chase (T1, 66 DAS; and T2, 88 DAS)*

P% was calculated as described in "Materials and Methods" and permitted the determination of the percentage of ^{15}N mobilized from the labeled rosettes and roots to the new organs that appeared between T0 and T1 and between T1 and T2. Values are the means and SEs of three plants. f.b., Flowering bud.

	RIL083			RIL272		
	Partitioning of ^{15}N, % P%(^{15}N), Mean	±SE	Percentage of ^{15}N Mobilized	Partitioning of ^{15}N, % P%(^{15}N), Mean	±SE	Percentage of ^{15}N Mobilized
T0 (f.b.)						
Roots	20.3	±1.0		25.3	±7.1	
Rosette	79.7	±1.0		74.7	±7.0	
T1 (7 d after f.b.)			Between T0 and T1			Between T0 and T1
Roots	20.3	±1.8	0	25.3	±2.2	0
Rosette	66.7	±1.3	12.6	62.1	±0.9	12.6
Flowering stem I	2.7	±1.6		3.3	±1.2	
Cauline leaves I	2.6	±0.6		2.6	±1.0	
Flowers I	7.7	±5.3		6.7	±3.0	
T2 (1 month after f.b.)			Between T1 and T2			Between T1 and T2
Roots	18.7	±0.8	1.5	24.1	±1.8	1.4
Rosette	42.6	±0.6	24.0	37.2	±4.9	24.9
Flowering stem I	6.6	±0.7		7.8	±0.9	
Flowering stem II	5.0	±2.0		9.0	±4.0	
Cauline leaves	12.9	±0.7		11.9	±3.0	
Siliques and flowers	14.2	±1.0		10.0	±1.0	

maintained at T1, because there was no ^{15}N mobilization from the roots to the rest of the plant for RIL083 and RIL272 between T0 and T1. Between T0 and T1, the ^{15}N exported to the new growing organs was only coming from the rosettes, and the level of the ^{15}N mobilized was similar in the two lines, reaching 12.6% of the whole plant ^{15}N and 16% of the ^{15}N contained in the rosette at T0. The ratio of ^{15}N translocated to the [stem I + cauline leaves + flowers] was similar in the two RILs and mainly dedicated to flowers that received almost 60% of the ^{15}N pool that was remobilized from the rosette, while the stem I and cauline leaves received 20% each.

Between T1 and T2, 1.5% of the whole plant ^{15}N was reallocated from the roots to the flowering stems and reproductive organs, while 24% of the whole plant ^{15}N (or 36% to 40% of ^{15}N contained in the rosettes at T1) was exported from the rosette to the flowering stems and reproductive organs. Remobilization from the rosettes mainly benefited the cauline leaves and the flower + silique compartments. The strength of these two sinks appeared slightly more powerful in RIL083 than in RIL272 (Table I).

Because there was no significant difference in the level of ^{15}N mobilized from the rosettes of the early-senescing line RIL083 and the late-senescing line RIL272, while the siliques and flowers sinks seemed to be slightly favored in RIL083, the question of grain filling was addressed. Hydroponic culture mode is not suitable to seed production. Culture on sand was then preferred. Culture on sand did not permit the harvest of roots; however, because the remobilization of ^{15}N from the roots measured in previous experiments appeared very weak, it was assumed that neglecting the root compartment will not drive large errors. For each RIL, four plants were cultivated in N-limiting conditions. The labeled $^{15}NO_3^-$ was provided to the plants in the watering solution, twice at 40 and 42 DAS, when the rosette growth was exponential. After ^{15}N uptake, sand was carefully rinsed several times with distilled water to remove the remaining labeled N. The transfer of the plants from short-day photoperiod to long-day photoperiod at 56 DAS induced flowering and reduced the difference of flowering time between the RILs. Plant material was collected at the end of the cycle when the whole plants were dry and seeds fully matured (i.e. around 140 DAS). The partition of dry matter (milligrams DW), total N (milligrams), and ^{15}N (micrograms) between the dry remains (rosette + stems + cauline leaves + siliques) and the seeds compartment was investigated (Table II).

At the end of their life cycle, the total biomass (DW) per plant was similar (around 800 mg/plant) for all the RILs, except RIL083, whose dry matter was slightly lighter. The total N and ^{15}N per plant were not different between the five RILs, thus showing that the N uptake was similar for all the plants and genotypes. However, the partitioning of dry matter, total N, and ^{15}N in the seeds was significantly different between RIL310 and the other RILs. Compared to other genotypes, RIL310 produced large vegetative biomass and very few seeds. For that reason, the quantity of ^{15}N mobilized to the seeds was also very low. Thus, except in the case of RIL310, the partitioning of ^{15}N in the seed

Table II. *Comparison of the partitioning of the DW (milligrams per plant), total N content (milligrams per plant), and total ^{15}N content (micrograms per plant) between total seeds, dry remains after seed harvest (named shoot), and whole plant*

The partitioning P% (in percentage of the whole plant) of the DW, the total N, and the ^{15}N of the seed compartments of the five RILs have been calculated from four individual plant repeats. For all the data, means and SES, $n = 4$, are presented.

	DW			Total N			^{15}N			P% in the Seeds		
	Shoot	Seeds	WP	Shoot	Seeds	WP	Shoot	Seeds	WP	P%(DW)	P%(N)	P%(^{15}N)
	mg			*mg*			*μg*			*% of WP*		
RIL310	786 ± 221	52 ± 20	838 ± 214	10.7 ± 3.3	2.0 ± 0.8	12.7 ± 2.8	41.4 ± 9.7	5.2 ± 2.2	46.6 ± 8.8	6.6 ± 3.4	16.4 ± 10.6	11.6 ± 5.1
RIL083	382 ± 70	231 ± 51	613 ± 119	3.3 ± 0.3	7.8 ± 1.9	11.13 ± 2.0	15.7 ± 2.9	32.0 ± 4.6	47.7 ± 4.0	37.5 ± 2.4	69.1 ± 6.5	67.1 ± 6.0
RIL232	577 ± 56	235 ± 15	812 ± 57	4.4 ± 0.6	8.0 ± 0.7	12.4 ± 0.9	16.8 ± 1.8	29.2 ± 2.9	46.0 ± 2.0	29.0 ± 2.5	64.3 ± 3.6	63.4 ± 4.5
RIL045	619 ± 123	200 ± 59	819 ± 66	7.4 ± 3.8	7.0 ± 1.8	14.4 ± 2.4	17.7 ± 7.7	30.9 ± 9.8	48.6 ± 9.6	25.0 ± 8.7	50.6 ± 16.5	63.6 ± 14.6
RIL272	512 ± 44	255 ± 19	767 ± 62	4.2 ± 0.3	9.3 ± 0.8	13.5 ± 0.9	15.3 ± 2.0	34.6 ± 7.9	49.9 ± 10.7	33.2 ± 1.0	68.5 ± 1.6	69.1 ± 2.2

compartment was similar between all the RILs, thus showing that ^{15}N remobilization to the seeds was as efficient in early- and late-senescing lines. Approximately 65% of the ^{15}N that was assimilated in rosettes during the vegetative phase (at 40 and 42 DAS) was remobilized for grain filling. The $P\%(N)_{seed}$ and the $P\%(^{15}N)_{seed}$ were not significantly different for all the RILs. This shows that the plants did not discriminate between ^{15}N and ^{14}N for grain filling.

Exp. 3 was carried out twice, and each repeat contained four plant replicates. This allowed us to test the correlation between the partition of dry matter [$P\%(DW)_{seeds}$] and the partitioning of ^{15}N [$P\%(^{15}N)_{seeds}$] in the seeds. The correlation between $P\%(DW)_{seeds}$ and $P\%(^{15}N)_{seeds}$ was high and repetitive: $R^2 = 0.826$ for the first experiment and $R^2 = 0.720$ for the second. This showed that the ratio between the source and the sink sizes was correlated with the level of the flux of N to the seeds.

DISCUSSION

To investigate the effect of senescence and leaf aging on the N remobilization process in Arabidopsis, the molecular physiology of five RILs from the Bay-0 × Shahdara population was investigated. These lines have been previously studied and analyzed for several N use efficiency and leaf-yellowing traits (Loudet et al., 2003; http://dbsgap.versailles.inra.fr/vnat/Documentation/33/DOC.html; Diaz et al., 2006) and for metabolic markers allowing senescence severity characterization (Diaz et al., 2005).

The determination of the biomass, amino acid content, and sugar content led us to confirm some correlations and characterizations that have been previously observed on the whole population in response to N limitation (Loudet et al., 2003; Diaz et al., 2005, 2006). In this article, we observed indeed that the early-senescing lines showed lower dry matter accumulation in their rosettes than late-senescing lines. This was consistent with the negative correlation found between traits at 35 DAS (vegetative stage) for leaf yellowing and dry matter level (Diaz et al., 2006).

We observed here that the NL of the early-senescing lines were more concentrated in protein and free amino acid than the NL of late-senescing lines. By contrast, they contained a lower amount of total sugars. The NL composed the major part of the rosette after 35 DAS. This opposite trend between early- and late-senescing genotypes was consistent with the positive correlation found between leaf-yellowing and total N concentration described in Diaz et al. (2006) and with the colocalization of the major quantitative trait loci (QTLs) found for N use efficiency and yellowing. It remains, however, to be explained why early-senescing lines accumulated more N and chlorophyll and less sugar in their NL than late-senescing lines. In addition, the reason why the chlorophyll content was higher in the NL of early-senescing lines while starch accumulation and dry matter were lower is unclear. One hypothesis is that the whole rosette of early-senescing lines has a lower carbon use efficiency.

The total N, amino acid, and protein concentrations measured in the NL and the 6FL decreased with aging in the five RILs. This trend can be attributed to the N dilution process already described for many plant species (Greenwood et al., 1990; Justes et al., 1994; Plénet and Lemaire, 2000). Soluble protein concentration decreased earlier and to a greater extent in the 6FL of the early-senescing lines, whereas the total N concentration decreased similarly over time between all the RILs. This suggested that N remobilization and proteolysis have been enhanced earlier and in the same time as senescence symptoms progressed. The measurement of NR and GDH activities suggested that N assimilation decreased and Glu catabolism increased with aging. The check point between the primary assimilation phase and the remobilization phase, as described by Masclaux et al. (2000), was around 40 DAS for all the lines. Determination of total GS activity was more informative and facilitated the monitoring of leaf senescence and the N remobilization process. The change in total GS is the result of both GS2 and GS1 fluctuations. Because GS2 is the most represented GS isoenzyme in the leaves, the decrease of total GS can be attributed to a decrease of GS2, as observed on the western blots and suggested by the down-regulation of *gln2*. The decrease of GS activity was detected sooner in early-senescing lines (as soon as 34 DAS for RIL310). In parallel with the decrease of assimilation transcripts like *cab*, *nia*, and *gln2*, the transcripts for the N remobilization enzymes like GS1 and GDH accumulated. This accumulation occurred

earlier in the early-senescing lines and paralleled senescence symptoms. In accordance with the accumulation of γ-aminobutyric acid observed by Diaz et al. (2005), we observed here the accumulation of the *gad2* transcripts with aging. While *gln1.1* and *gln1.2* transcripts accumulated, increased GS1 protein content was also observed. The good correlation between *gln1.2* and *gln1.1* induction, GS1 accumulation, and leaf senescence severity suggested that the N remobilization was more efficient and occurred earlier in the early-senescing lines. In addition, the similar increase of *gdh2* expression and GDH activity with aging suggests that GDH participate in amino acid degradation and recycling in Arabidopsis (Masclaux-Daubresse et al., 2006).

Free amino acids present in senescing leaves are supposed to be released from the intense proteolytic activity induced with aging (Brouquisse et al., 2000). Indeed, we observed that Rubisco, which is the largest N storage protein, decreased with aging. Antibodies raised against the tobacco CND41 protein allowed us to detect a signal in the 6FL extracts that increased with aging and paralleled the decrease of Rubisco protein. While Rubisco decrease was stronger in early-senescing lines, the CND41-like protein was much more abundant in the leaves of early-senescing lines. This CND41 homolog proved then to be a good marker for leaf senescence severity, and its large accumulation in parallel with Rubisco decrease suggests that this protease has an important role in N remobilization in Arabidopsis (Kato et al., 2005a, 2005b).

All together, the results of the molecular physiology of the five RILs showed that N remobilization markers were expressed earlier in the early-senescing lines. The remaining question was then to determine if the early-senescing lines mobilize N more efficiently than late-senescing lines.

To address this question, ^{15}N labeling and tracing experiments were performed. The results showed that NRE was different depending on the source/sink model considered. The labeling protocols used here allowed us to determine the remobilization of N from the roots and the shoot compartments to the sink organs that appeared during the chase period. The new organs formed during the chase period, such as NL, flowering stems, and seeds, were certainly not the lone sink for N remobilization, because it is known that roots can also be sink (Rossato et al., 2002). We cannot exclude the possibility that during the chase period, roots also gained ^{15}N from the first leaves. However, such a ^{15}N flux to the roots was not detected here, and the imbalance between root gain and root export only quantified root export. Then results showed that the ^{15}N mobilized and exported from the roots was less than the amount mobilized from the leaves. The most striking result was that the level of ^{15}N mobilized from leaf to leaf during the vegetative phase of the rosette growth was higher in early-senescing lines than in late-senescing lines. N remobilization during vegetative development of the rosette was then clearly dependent on the senescence symptoms severity. By contrast, the level of ^{15}N remobilized from the whole rosette to the flowering organs during the reproductive phase did not differ between the lines. The proportion of ^{15}N assimilated during the vegetative phase of leaf development and mobilized to the seeds and flowering stems was not related to the leaf senescence phenotype. For all the lines, except RIL310, approximately 65% of the ^{15}N absorbed during the vegetative growth was remobilized to the seeds. The variation between the lines RIL045, RIL272, RIL083, and RIL232 was weak. In RIL310, the amount of N remobilized to the seeds was very low, and this is certainly a result of the low fitness of this line. Using all the data available on the five lines, a good correlation was found between the partitioning of dry matter in the seeds and the partitioning of ^{15}N in the seeds. This indicated that the efficiency of N remobilization to the grain was certainly controlled by the respective sizes of the sink and source compartments. The RIL310, which is a late-flowering line, has favored vegetative growth rather than reproduction.

As a result, we conclude that leaf senescence influences NRE at the vegetative stage only, emphasizing that leaf senescence and rosette senescence have to be distinguished as sequential senescence occurring during the vegetative rosette development and a monocarpic senescence that occurs at the flowering stage. The existence of both sequential and monocarpic senescence in Arabidopsis depends on genotype and environment. Monocarpic senescence is more easily observed when plants are grown in a long-day photoperiod to favor flowering and is related to the whole rosette longevity rather than to individual leaf senescence symptoms (Levey and Wingler, 2005). Sequential leaf senescence observed during the vegetative stage varies with genotypes and can be more easily observed when plants are grown in short-day photoperiod and, for example, under N-limiting nutrition (Diaz et al., 2006).

Monocarpic and sequential senescence are certainly not controlled by the same genetic basis (Luquez et al., 2006) and do not have the same influence on NRE. Diaz et al. (2006) showed that the most important QTLs to explain individual leaf senescence under limiting N nutrition colocalize with N use efficiency QTLs measured at vegetative stage. In this article, the absence of genetic variation for the NRE to the seeds questions the pertinence of searching for N remobilization QTLs in the Bay-0 × Shahdara population. Studying NRE traits using a population of accessions, or core collections of RILs, would be necessary to assess correlation between senescence, NRE, and harvest index [P%(DW)] traits.

MATERIALS AND METHODS

Plant Material and Growth Conditions for Physiological Study

The five lines RIL310, RIL272, RIL232, RIL083, and RIL045 selected from the Bay-0 × Shahdara RIL population have been previously described and

characterized by Diaz et al. (2005). Plants were grown as described by Diaz et al. (2005) under nitrate-limiting conditions and in short days (light/dark cycle 8 h/16 h) and photosynthetic photon flux density of 160 μmol m^{-2} s^{-1}. The pots were watered three times per week by immersion of the base of the pots in a solution, pH 5.5, containing 3 mM nitrate (Diaz et al., 2005). About 20 d after sowing, the five RILs had formed six leaves plus cotyledons. Diaz et al. (2005) have observed that the time when the 6FL emerged was similar for all the RILs, whereas the date of emergence of further leaves was different. As physiological studies require a lot of plant material, we decided to use the 6FL of the rosettes. For metabolic and molecular analysis, the 6FL of four or six rosettes were dissected every 3 or 4 d and pooled. At each harvesting time, four different bulks of 6FL were harvested per RIL between 10 and 11 AM and stored at –80°C before further experiments. The remaining part of the rosette, called NL and consisting of the young leaves that emerged after the 6FL, was also collected and stored.

Hydropony and ^{15}N Tracing

Three different labeling experiments were performed to determine ^{15}N remobilization: (1) from leaf to leaf during the vegetative phase of rosette growth (Exp. 1); (2) from rosette to flowering organs during the reproductive phase (Exp. 2); and (3) for seed filling at the end of plant cycle (Exp. 3).

Exp. 1 and Exp. 2 Were Conducted Using Hydroponically Grown Plants

Seeds were vernalized in agar 0.1% for 48 h at 4°C. The seeds were then sown directly on the top of modified Eppendorf tubes (0.5-mL Eppendorf tubes from which the bottom was cut and top removed) filled with 0.8% agar (Kalys) melted in a dilution (1:1 with distilled water) of the ^{15}N nutritive solution. The composition of the ^{15}N nutritive solution was 0.25 mM KH_2PO_4, 0.321 mM K_2SO_4, 0.25 mM $MgSO_4$, 0.1 mM $K^{15}NO_3$ (2.5% enrichment), and 0.25 mM $CaCl_2$. The tubes were positioned on floating rafts transferred on diluted (1:1) ^{15}N nutritive solution in a growth chamber under the following environmental conditions: 8-h-light/16-h-dark cycle, light intensity of 160 μmol s^{-1} m^{-2}, temperature of 21°C/17°C, and hygrometry 85%. After 1 week, the diluted (1:1) ^{15}N nutritive solution was replaced by full ^{15}N undiluted nutrient solution. The labeling period of time varied between Exp. 1 and Exp. 2 and ended with the T0 of harvest. Exp. 1 was conducted on the five RILs, while Exp. 2 was conducted on only RIL272 and RIL083.

For Exp. 1, T0 was 27 DAS, when rosettes have emerged 11FL. At T0, six plants were harvested to form root and 11FL labeled samples. For the six remaining plants, which had not been harvested and passed the chase period, all the leaves that emerged during the pulse period were marked, even if very small, with a small spot using white pen corrector to further detect the 11FL. At 27 DAS (T0), the ^{15}N nutritive solution was replaced by unlabeled ^{14}N nutritive solution with the same nutrient composition, except that $K^{15}NO_3$ was replaced by $K^{14}NO_3$. Before transferring plants on the unlabeled solution, roots and all material were carefully rinsed using permutated water. A second harvest was done at T1, 37 DAS, when six to seven NL emerged during the chase period. Plants were dissected as roots, 11FL, and NL. Exp. 1 was carried out twice.

In Exp. 2, the ^{15}N and ^{14}N nutritive solutions were the same as in Exp. 1. The end of the pulse period at T0 was 59 DAS, when RIL272 and RIL083 emerged concomitantly flowering buds. At T0, three labeled plants were harvested to form root and whole-rosette T0 labeled samples. For the remaining plants, the ^{15}N nutritive solution was replaced by unlabeled ^{14}N nutritive solution. As for Exp. 1, roots and all material were carefully rinsed using distilled water before transferring plants to the unlabeled solution. At T1, 66 DAS, the roots, rosettes, and the newly appeared organs of three plants were dissected. The new organs were separated as the primary flowering stem (I), cauline leaves (I) on the primary flowering stem, and the flowers (I) carried on the primary flowering stem. At T2, 88 DAS, three remaining plants were dissected to form the roots, the rosette, the primary flowering stem (I), the secondary flowering stem (II), the cauline leaves, and the siliques plus flowers carried on the flowering stems I and II.

Exp. 3 Was Carried Out Using Plants Grown on Sand

Seeds of the five RILs were vernalized in agar 0.1% for 48 h at 4°C and sown on sand. Plants were grown in a growth chamber under the following environmental conditions: light intensity, 160 μmol s^{-1} m^{-2}; temperature, 21°C/17°C; hygrometry, 85%; and 8-h-light/16-h-dark cycle, for 56 d. After 56 DAS, plants were transferred to long-day conditions (16-h-light/8-h-dark cycle) to induce flowering. The pots were watered three times per week by immersion of the base of the pots in a solution, pH 5.5, containing 3 mM nitrate, 2.75 mM potassium, 0.5 mM calcium, 0.7 mM chloride, 0.25 mM phosphate, 0.25 mM sulfate, 0.25 mM magnesium, and 0.20 mM sodium. At two ^{15}N uptake time points, 40 and 42 DAS, the unlabeled watering solution was replaced by a ^{15}N-containing solution that had the same nutrient composition except that $^{14}NO_3$ was replaced by $^{15}NO_3$ 10% (w/w) enrichment. Plants were harvested at the end of their cycle when the total seeds were matured and the rosette dry. Samples were separated as dry [rosette + stem + cauline leaves + siliques], named "shoot," and total seeds. Four replicates of each RIL were harvested and the experiment was carried out twice.

For all the experiments, unlabeled samples were harvested to determine the ^{15}N natural abundance.

Determination of Total N Content and ^{15}N Abundance and Partition

In all the labeling experiments, after drying and weighing each plant part, material was ground to obtain homogenous fine powder. A subsample of 1,000 to 2,000 μg was carefully weighed in tin capsules to determine total N content and ^{15}N abundance using an elemental analyzer (roboprep CN; PDZ Europa Scientific) coupled to an isotope ratio mass spectrometer (Twenty-twenty; PDZ Europa Scientific) calibrated measuring natural abundance. The ^{15}N abundance of samples was calculated as atom percent and defined as $A\% = 100(^{15}N)/(^{15}N + {}^{14}N)$ for labeled plant samples and for unlabeled plant controls (Acontrol% was approximately 0.3660). The ^{15}N enrichment of the plant material was then defined as (Asample% − Acontrol%). The absolute quantity of ^{15}N contained in the i sample was Qi = DWi (Ai% − Acontrol%)%Ni, with %Ni = [mg N × (100 mg DWi)]$^{-1}$. The Q value of the wp can be measured and Qwp = $\sum$Qi. The partition P% of ^{15}N in the organ i was calculated as $P\%(^{15}N)i = [(Ai\% - Acontrol\%)DWi\ \%Ni]/[(Awp\% - Acontrol\%)DWwp\ \%Nwp] = Qi/Qwp$.

Metabolite Extraction and Analysis

Amino acids and NH_4^+ were determined after extraction in 2% solution of 5-sulfosalicylic acid (50 mg FW mL^{-1}) by the Rosen colorimetric method using Gln as a reference (Rosen, 1957). Sugars were determined after ethanolic extraction (Loudet et al., 2003). Suc and hexoses were determined as described by Masclaux-Daubresse et al. (2002) in supernatants. Starch content was determined from pellets (Masclaux-Daubresse et al., 2002).

Enzymatic Assays

Enzymes were extracted from frozen leaf material stored at −80°C. Nitrate reductase was extracted and the maximal extractable activity measured as described by Ferrario-Méry et al. (1997). GS was measured according to the method of O'Neal and Joy (1973). The NADH- and NAD^+-dependent GDH were measured as described by Turano et al. (1996), except that the extraction buffer was the same as for GS.

Chlorophyll and Total Protein Determinations

Chlorophyll content was determined in crude leaf extracts used for GS activity (Arnon, 1949). Soluble protein content was determined in crude leaf extracts used for GS activity using a commercially available kit (Coomassie Protein assay reagent; Bio-Rad).

Gel Electrophoresis, Western-Blot Analysis, and Gel-Staining Procedure

Proteins were extracted in HEPES (50 mM, pH 7.5), $MgCl_2$ (2 mM), EDTA (0.5 mM), dithiothreitol (2 mM), and Triton X-100 0.1% buffer. Proteins from three different extracts were pooled and separated by SDS-PAGE (Laemmli, 1970). The percentage of polyacrylamide in the running gels was 8% for GS and 12% for Rubisco and CND41. An equal amount of protein (10 μg for GS, 20 μg for CND41, and 6 μg for Rubisco) was loaded in each track. Denaturated proteins were electrophoretically transferred to nitrocellulose membranes or

directly stained with Coomassie Blue for Rubisco detection. Polypeptide detection was performed using polyclonal antiserum raised against tobacco (*Nicotiana tabacum*) GS2 (Becker et al., 1992) and CND41 (Kato et al., 2004). Relative GS2, GS1, CND41, and Rubisco protein amounts were determined by densitometric scanning of western-blot membranes or stained gels and quantification using the Fujifilm FLA5000 phosphoimager and the Multi-Gauge Fujifilm image analyzer (Fujifilm).

Extraction of Total RNA and Northern-Blot Analysis

Total RNA was extracted from plant material stored at −80°C. Northern-blot analysis was performed as described previously (Masclaux et al., 2000). ^{32}P-labeled probes were used for mRNA detection. Specific probes raised against *gln2* (*At5g35630*), *gln1.1* (*At5g37600*), and *gln1.2* (*At1g66200*) were obtained through PCR amplification as described by Oliveira and Coruzzi (1999). Specific probe raised against *gdh2* (*At5g07440*) was obtained using the 1.4-kb cDNA *Sal*I/*Eco*RI inserts purified from the 188II23T7 EST clone provided by the Arabidopsis Biological Resource Center (ABRC; Columbus Ohio). The *gad2* (*At1g65960*)-specific probes were kindly provided by Dr. Nicolas Bouché (INRA, Versailles, France) and obtained from the cognate ABRC EST vectors after digestion by *Kpn*I/*Hin*dIII restriction enzymes and purification of cDNA. The *CAB* probe was kindly provided by Dr. Dolores Abarca (Abarca et al., 2001). The 18S rRNA probe was the same as used by Masclaux et al. (2000). High stringency hybridization conditions were used for all the probes.

Sequence data from this article can be found in the GenBank/EMBL data libraries under accession numbers NM10291, NM123119, NM122954, NM001125712, NM108268, NM103364, and NM122728.

ACKNOWLEDGMENTS

Thanks to Marie-Paule Bataillé (UMR INRA-UCBN, University of Caen, France) for technical assistance in ^{15}N content determination. The authors thank Dr. Nicolas Bouché, Dr. Dolores Abarca (University of Madrid, Madrid), and Dr. Bertrand Hirel (INRA, Versailles, France) for providing molecular probes or antibodies. The authors thank the ABRC, which provided the 188II23T7 EST plasmid. Thanks to Dr. Christophe Simon (Riken, Yokohama Institut, Genomic Science Center, Japan) and Dr. Nicolas Bertin (Riken) for proofreading of the manuscript.

Received March 17, 2008; accepted April 26, 2008; published May 8, 2008.

LITERATURE CITED

Abarca D, Martin M, Sabater B (2001) Differential leaf stress responses in young and senescent plants. Physiol Plant **113:** 409–415

Arnon DI (1949) Copper enzymes in isolated chloroplasts. Polyphenol oxidase in *Beta vulgaris* L. Plant Physiol **24:** 1–15

Becker TW, Caboche M, Carrayol E, Hirel B (1992) Nucleotide sequence of a tobacco cDNA encoding plastidic glutamine synthetase and light inducibility, organ specificity and diurnal rhythmicity in the expression of the corresponding genes of tobacco and tomato. Plant Mol Biol **19:** 367–379

Bernhard WR, Matile P (1994) Differential expression of glutamine synthetase genes during senescence of Arabidopsis rosette leaves. Plant Sci **98:** 7–14

Brouquisse R, Masclaux C, Feller U, Raymond P (2000) Protein hydrolysis and nitrogen remobilisation in plant life and senescence. *In* P Lea, JF Morot-Gaudry, eds, Plant Nitrogen. Springer, INRA Editions, Paris, pp 275–293

Brugière N, Dubois F, Masclaux C, Sangwan RS, Hirel B (2000) Immunolocalization of glutamine synthetase in senescing tobacco (*Nicotiana tabacum* L.) leaves suggests that ammonia assimilation is progressively shifted to the mesophyll cytosol. Planta **211:** 519–527

Buchanan-Wollaston V, Earl S, Harrison E, Mathas E, Navabpour S, Page T, Pink D (2003) The molecular analysis of leaf senescence: a genomics approach. Plant Biotechnol J **1:** 3–22

Cabello P, Agüera E, de la Haba P (2006) Metabolic changes during natural ageing in sunflower (*Helianthus annuus*) leaves: expression and activity of glutamine synthetase isoforms are regulated differently during senescence. Physiol Plant **128:** 175–185

Diaz C, Purdy S, Christ A, Morot-Gaudry JF, Wingler A, Masclaux-Daubresse C (2005) Characterization of markers to determine the extent and variability of leaf senescence in Arabidopsis. A metabolic profiling approach. Plant Physiol **138:** 898–908

Diaz C, Saliba-Colombani V, Loudet O, Belluomo P, Moreau L, Daniel-Vedele F, Morot-Gaudry JF, Masclaux-Daubresse C (2006) Leaf yellowing and anthocyanin accumulation are two genetically independent strategies in response to nitrogen limitation in Arabidopsis. Plant Cell Physiol **47:** 74–83

Ferrario-Méry S, Thibaud M-C, Bettsche T, Valadier M-H, Foyer C (1997) Modulation of carbon and nitrogen metabolism, and of nitrate reductase, in untransformed and transformed *Nicotiana plumbaginifolia* during CO_2 enrichment of plants grown in pots and in hydroponic culture. Planta **202:** 510–521

Greenwood D, Lemaire G, Gosse G, Cruz P, Draycott A, Neeteson J (1990) Decline in percentage N of C3 and C4 crops with increasing plant mass. Ann Bot (Lond) **66:** 425–436

Guo Y, Cai Z, Gan S (2004) Transcriptome of Arabidopsis leaf senescence. Plant Cell Environ **27:** 521–549

Ishida H, Shimizu S, Makino A, Mae T (1998) Light-dependent fragmentation of the large subunit of ribulose-1,5-biphosphate carboxylase/oxygenase in chloroplasts isolated from wheat leaves. Planta **204:** 305–309

Justes E, Mary B, Meynard JM, Machet JM, Thelier-Huche L (1994) Determination of a critical nitrogen dilution curve for winter wheat crops. Ann Bot (Lond) **74:** 397–407

Kato Y, Murakami S, Yamamoto Y, Chatani H, Kondo Y, Nakano T, Yokota A, Sato F (2004) The DNA-binding protease, CND41, and the degradation of ribulose-1,5-bisphosphate carboxylase/oxygenase in senescent leaves of tobacco. Planta **220:** 97–104

Kato Y, Saito N, Yamamoto Y, Sato F (2005a) Regulation of senescence by aspartic protease: CND41 in tobacco and CND41 homologues in Arabidopsis. *In* A van der Est, D Bruce, eds, Proceedings of the Photosynthesis Congress 2004, Photosynthesis: Fundamental Aspects to Global Perspectives. Alliance Communications Group, Lawrence, KS, pp 821–823

Kato Y, Yamamoto Y, Murakami S, Sato F (2005b) Post-translational regulation of CND41 protease activity in senescent tobacco leaves. Planta **222:** 643–651

Laemmli UK (1970) Cleavage of structural proteins during the assembly of the head of bacteriophage T4. Nature **227:** 680–685

Leopold AC (1961) Senescence in plant development. Science **134:** 1727–1732

Levey S, Wingler A (2005) Natural variation in the regulation of leaf senescence and relation to other traits in Arabidopsis. Plant Cell Environ **28:** 223–231

Loudet O, Chaillou S, Merigout P, Talbotec J, Daniel-Vedele F (2003) Quantitative trait loci analysis of nitrogen use efficiency in Arabidopsis. Plant Physiol **131:** 345–358

Luquez VM, Sasal Y, Medrano M, Martin MI, Mujica M, Guiamet JJ (2006) Quantitative trait loci analysis of leaf and plant longevity in Arabidopsis. J Exp Bot **57:** 1363–1372

Martin A, Belastegui-Macadam X, Quillere I, Floriot M, Valadier MH, Pommel B, Andrieu B, Donnison I, Hirel B (2005) Nitrogen management and senescence in two maize hybrids differing in the persistence of leaf greenness: agronomic, physiological and molecular aspects. New Phytol **167:** 483–492

Masclaux C, Valadier M, Brugière N, Morot-Gaudry J, Hirel B (2000) Characterization of the sink/source transition in tobacco (*Nicotiana tabacum* L.) shoots in relation to nitrogen management and leaf senescence. Planta **211:** 510–518

Masclaux-Daubresse C, Reisdorf-Cren M, Orsel M (2008) Leaf nitrogen remobilization for plant development and grain filling. Plant Biol (in press)

Masclaux-Daubresse C, Reisdorf-Cren M, Pageau K, Lelandais M, Grandjean O, Kronenberger J, Valadier MH, Feraud M, Jouglet T, Suzuki A (2006) Glutamine synthetase/glutamate synthase pathway and glutamate dehydrogenase play distinct roles for sink/source nitrogen cycle in tobacco (*Nicotiana tabacum* L.). Plant Physiol **140:** 444–456

Masclaux-Daubresse C, Valadier MH, Carrayol E, Reisdorf-Cren M, Hirel B (2002) Diurnal changes in the expression of glutamate dehydrogenase and nitrate reductase are involved in the C/N balance of tobacco source leaves. Plant Cell Environ **25:** 1451–1462

Nakano T, Murakami S, Shoji T, Yoshida S, Yamada Y, Sato F (1997) A novel protein with DNA binding activity from tobacco chloroplast nucleoids. Plant Cell **9:** 1673–1682

Oliveira IC, Coruzzi GM (1999) Carbon and amino acids reciprocally modulate the expression of glutamine synthetase in Arabidopsis. Plant Physiol **121:** 301–309

O'Neal D, Joy KD (1973) Glutamine synthetase of pea leaves. I. Purification, stabilisation and pH optima. Arch Biochem Biophys **159:** 113–122

Plénet D, Lemaire G (2000) Relationship between dynamics of nitrogen uptake and dry matter accumulation in maize crops: determination of critical N concentration. Plant Soil **216:** 65–82

Rosen H (1957) A modified ninhydrin colorimetric analysis for amino acids. Arch Biochem Biophys **67:** 10–15

Rossato L, Le Dantec C, Laine P, Ourry A (2002) Nitrogen storage and remobilization in *Brassica napus* L. during the growth cycle: identification, characterization and immunolocalization of a putative taproot storage glycoprotein. J Exp Bot **53:** 265–275

Schulze W, Schulze ED, Stadler J, Heilmeier H, Stiit M, Mooney HA (1994) Growth and reproduction of Arabidopsis in relation to storage of starch and nitrate in the wild-type and in starch-deficient and nitrate-uptake-deficient mutants. Plant Cell Environ **17:** 795–809

Turano FJ, Dashner R, Upadhayaya A, Caldwell CR (1996) Purification of mitochondrial glutamate dehydrogenase from dark-grown soybean seedlings. Plant Physiol **112:** 1357–1364

van der Graaff E, Schwacke R, Schneider A, Desimone M, Flugge UI, Kunze R (2006) Transcription analysis of Arabidopsis membrane transporters and hormone pathways during developmental and induced leaf senescence. Plant Physiol **141:** 776–792